Archives of Materials Science and Engineering

Volume 83
Issue 2
February 2017
Pages 49-67

International Scientific Journal
published monthly by the
World Academy of Materials
and Manufacturing Engineering

Identification of mechanical parameters of bone tissue as a base of numerical simulation in medicine

A. John, G. Kokot
Institute of Computational Mechanics and Engineering, Silesian University of Technology,
ul. Konarskiego 18a, 44-100 Gliwice, Poland
Corresponding e-mail address: antoni.john@polsl.pl; grzegorz.kokot@polsl.pl

ABSTRACT

Purpose: The aim of the paper is to show the new possibility of evaluation of bone tissues properties in experiment and next the numerical simulation and verification of selected problems.

Design/methodology/approach: The lifestyle that has been favored lately has led to unfavorable changes in the human body. This is manifested mainly by joint anomalies and changes in the structure of bone tissue. The scientists try to aid the healing and rehabilitation systems. It is possible to prepare a numerical model of complex biomechanical structures using advanced FE systems. The process of modeling is one of the most important steps of this research and assignment of material data influences on the precision of obtained results. The classic measurement methods with particular emphasis on their application in the study of bone, taking into account the advanced methods for measuring displacement are applied (DIC, nanoindentation). Also QCT combined with evolutionary methods gives interesting results in identification of material parameters Numerical simulations are verified in experiment.

Findings: Obtained results allow to compare the displacement and strain from experiment and numerical simulation. From numerical simulation, after FEM analysis we obtained full set of mechanical parameters useful in planning of surgical intervention (THA, pelvis reconstruction), aided the diagnostic in risky state and design of prosthesis.

Research limitation/implications: The precision of identification of material parameters depend on many parameters and influences on the precision of the results from numerical simulation. Research is conducted mainly on preparations and not on living tissue. The target should be in-vivo noninvasive measurement.

Originality/Value: Combination of numerical simulation and experimental research is needed to obtain correct results and broaden the spectrum of relevant parameters necessary to support surgical and rehabilitation. Both approaches require modern equipment and advanced testing methods.

Keywords: Bone tissues properties evaluation; Mechanical tests; DIC; Nanoindentation; QCT; Numerical simulation; Advanced FEM; Experimental verification

Reference to this paper should be given in the following way:

A. John, G. Kokot, Identification of mechanical parameters of bone tissue as a base of numerical simulation in medicine, Archives of Materials Science and Engineering 83/2 (2017) 49-67.

MONOGRAPH

1. Introduction

The last time a sedentary way of life is amplified by poor quality of food and watching television instead of doing any sport etc. This conditions are leading to bad state of human body already in early time of life. It may lead to damage of such parts of human body like joints rather in normal condition of functionality, not only in high overloaded states. The reason for such state it could be weakening of bone, cartilage and synovial liquid.

The scientists try to aid the healing and rehabilitation systems. Advanced FE systems make it possible to prepare a numerical model of complex biomechanical structures - especially with respect to joints in human locomotion system. It is particular important when the THA operation is performed and the artificial acetabulum is fitted. Very often before and after operations the knowledge of the stress and strain distribution in the pelvic joint (pelvic bone and femur) is needed.

The process of modelling is one of the most important steps of this research. The precision of preparing the model influences meaningfully the precision of the results and time of solving the task by computer system and it could be divided into:

1. Preliminary preparation of geometry based on filtered CT scan data.
2. Division model to finite elements.
3. Assignment of material data.
4. Assignment of boundary condition.
5. Job analysis and interpretation of results.

The first part of our investigation concern determination of material parameters of bone tissue in experiment and the second part concern the numerical simulation and verification of selected problems.

2. Determination of material parameters

The basic information concern material properties of bone tissues we can find in the literature. The greatest source of information are the works of Cowin [1], An and Draughn [2] and Keaveny et al. [3]. Unfortunately, most of these works show results from traditional measurement methods. Many papers concern transformation data from CT or QCT (HU units) to material parameter as Young modulus (Ashman and Rho [4], Boutroy et al. [5], Helgeson et al. [6], Hodskinson and Currey [7], Keyak et al. [8,9], Pistoia et al. [10], Rho et al. [11]). The basis for testing of bone elastic properties (Young and Kirchhoff modulus, Poisson ratio) is a known mechanical tests like tension or compression, where during the cross head movement the force-displacement curve is registered (Feng and Jasiuk [12], Garnier et al. [13], Keaveny et al. [14,15], Keller [16], Öchsner and Ahmed [17], Reilly and Burstein [18], Sanyal et al. [19]). Torsion load is applied very rare (Garnier et al. [13], Kasra and Grympas [20]). Also three or four point bending test is performed. However using this methods we often encounter difficulties, which are mostly connected with displacement measurement, low precision and accuracy. This is connected with:

- the small specimen size,
- complicated mounting way,
- porous structure of the tested material,
- specimen condition (often under wet condition).

This had been main reasons that research on the using much more precise methods for evaluation of bone tissues mechanical properties have been undertaken.

The other thing is the hierarchical structure of the bone which strongly influence on the mechanical properties on the macro- and micro level. One can find in the literature so-called structural Young modulus, which describes behavior on the macro level and Young modulus for the single trabecula (Hanned et al. [21], Keaveny and Yeuh [22], Makowski et al. [23], Norman et al.[24], Rho et al. [25], van Rietbergen et al. [26], Vaughan et al. [27], Wang et al. [28,29]). Those values differ widely. Most of values presented in the literature were determine for macrostructure what is not enough in many cases of undertaken analysis and simulations (like for example remodelling). Our previous works with the modern experimental methods like DIC and nanoindentation have led to undertake the research on the possibility of using them in the field of biomechanics for evaluation of bone tissues mechanical properties.

The new possibility of evaluation of bone tissues properties give also intensively developing methods based on quantitative micro computed tomography μQCT and application of computational engineering methods in particular numerical simulations and evolutionary methods applied in the numerical identification of material parameters (Binkowski et al. [30-32], Cyganik et al. [33,34], Christen et al. [35], Ebenstein and Pruitt [36], Fan and Rho [37], Janca et al. [38], John and Kokot [39-41], John and Kuś [42], John et al.[43], Kokot et al. [44,45], Rezende et al. [46], van Rietbergen [47], Vilaypphiou et al. [48]). New methods for evaluation of the bone tissues mechanical properties and the stress-strain characteristics for bone structure also taking into account its microstructure. It could be done by combining the classical mechanical experimental methods with the new methods of the displacement measurement and combining the numerical simulation with the experimental methods.

The important thing is the displacement measurement. The simplest measurement is provided by the testing machine, the so-called measurement of the crosshead movement. However, it is characterized by rather large inaccuracy in the case of bone tissue. A significant improvement is achieved by the use of extensometers, however, due to the porous structure of the material and the small size of samples their application is also limited. Better results of the research provide optical methods, such as holographic interferometry and speckle photography. They provide non-contact measurement what is a significant advantage in the study of the bone structure. Although these methods have limitations associated with the registration of measurement (spot measurement, poor camera, no extensive software, poor digitization process), their use greatly expanded the accuracy and quality of the measurements.

Currently being developed optical methods of measurement of displacements and deformations, using advances in recording and processing of digital images, provide an online view of the field of displacements and deformations of the tested structure. Computer aided measurement allows to record and observe phenomena such as the concentration of deformation or crack formation and propagation. Other interesting problems concern that area one can find in the papers [9,22,27,28,49-59].

This article presents the classic measurement methods with particular emphasis on their application in the study of bone, taking into account the methods for measuring displacement and selection of samples for testing.

2.1. Digital Image Correlation

The applied so far optical methods or strain gauges for displacement or strain measuring in the bone tissues allow measurements only in the specified points of the structure. There is no wider information about the methods for accurate analysis of the local deformation especially on the level of microstructure. Here, as the helpful method we can apply the Digital Image Correlation.

The Digital Image Correlation (DIC) is an optical full-field technique for non-contact, 3D deformation measurements, where the high contrast speckle pattern applied onto the surface of the sample is observed by the CCD cameras during loading (Fig. 1). DIC as a tool for surface deformation measurements has found widespread use and acceptance in the field of experimental mechanics. The method is known to reconstruct displacements with subpixel accuracy and tangential surface strains in the sub-millistrain range. The algorithm of the DIC is based on the pseudo-affine transformation, which is described in [60,61] (materials of the Dantec Dynamics).

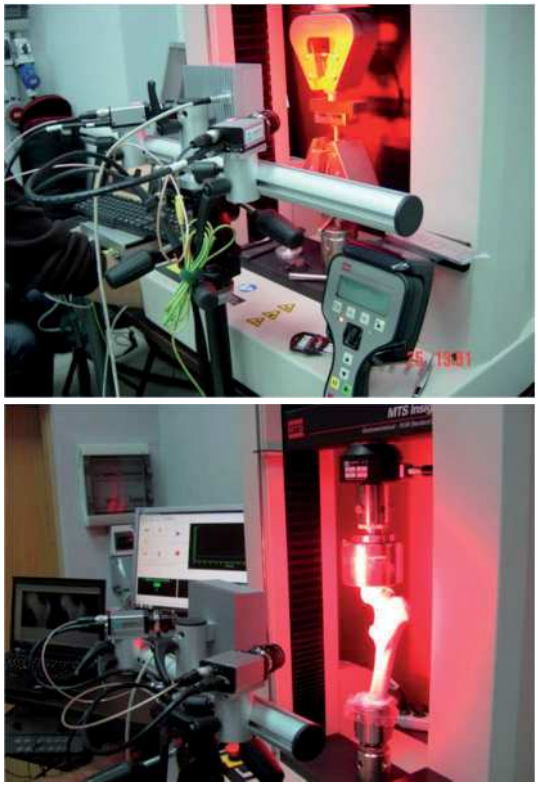

Fig. 1. The testing stand with the DIC

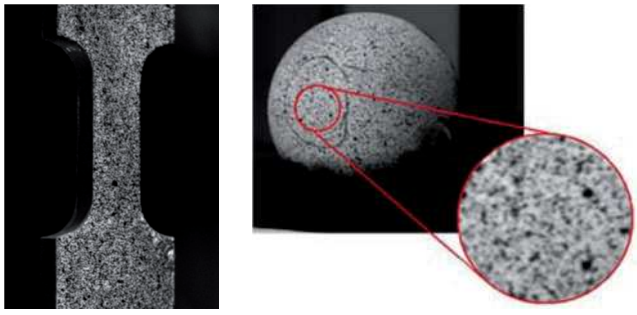

Fig. 2. The samples with special speckle pattern [60]

Using the DIC required some additional work such as determination of testing parameters and particularly choosing the specimens preparing method. This is the small disadvantage of this method – the covering the surface of the measured object with special speckle pattern (Fig. 2). For testing the testing stand was prepared by combining the DIC system with universal MTS testing machine. Data, which are obtained during test are collected and then analysed by specialized software. Data can also be analysed in a real time. The great advantage of this method is achieving the results on the whole specimen surface as the colours maps. Specialized software is used to analysing

the captured images during deformation and recalculation them to the form of the displacements/strains field (Fig. 3) which can be directly compare to results from the FE analysis. This is the great opportunity to direct validation of the numerical models.

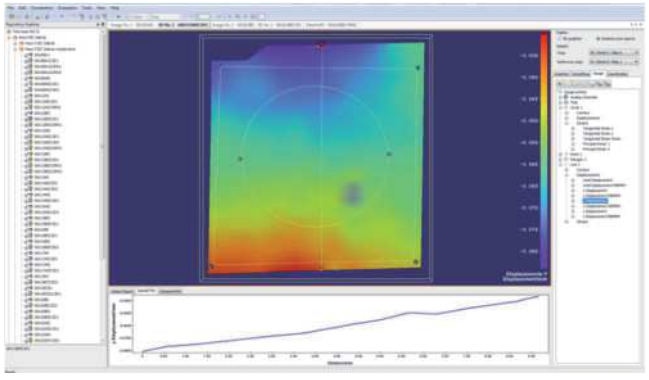

Fig. 3. Scan from Istria 4D – software for data aquisition and results postprocessing (cubic sample, compression test, displacement map)

In the conducted research the DIC system was combined with the classical experimental tests (tension/ compression, three point bending). Such combination considerably enhances possibility in evaluating the mechanical properties of bone tissues, particularly at the macrostructure level (John and Kokot [39], Kokot et al. [44,45], Sztefek et al. [62], Verhulp et al. [63]).

2.2. Compression test

One of the base test is tension or compression test. As most of the human skeleton parts work in compression condition the compression test is the mostly used test in bone tissue testing. The test is directly taken from experimental mechanics where sample is putted between two stiff platens and is compress with applied load. The typical testing stand is presented in the Fig. 4a and tested samples in the Fig. 4b and 4c.

Due to the nature of the tested material the sample dimensions deviate from the recommendations of code for common materials. It is understood that the tensile test is carried out on samples of cylindrical or rectangular shapes and compression test on the cubic shape samples. Detailed discussion of sampling, dimensions and their impact on the results is presented in the papers [1-3,12].

The typical disadvantages are the sample mounting and displacement measurements. In the case of the cylindrical samples they are often planted in the resin. But the most serious difficulties are mostly connected with displacement measurement and low precision and accuracy of results. This is due to small specimen size, complicated mounting way and porous structure of the tested material, often additionally under wet condition. The other thing is the hierarchical structure of the bone which strongly influence on the mechanical properties on the macro- and micro level. Typical compression load-extension and stress-strain curve for the spongy bone are presented in the Fig. 5 (own research).

As it was mention previous, according to prepared procedure the compression test for the cancellous bone wit DIC was performed. Testing stand shows Fig. 6 and obtained value of Young modulus for selected sample shows Fig. 7. A sample extracted from a human femur head and with special speckle pattern shows Fig. 8. Selected stress-strain curve for tested samples is presented in Fig. 9. You should pay attention to the curve character. It has a large linear-elastic range, with a short plastic deformation part.

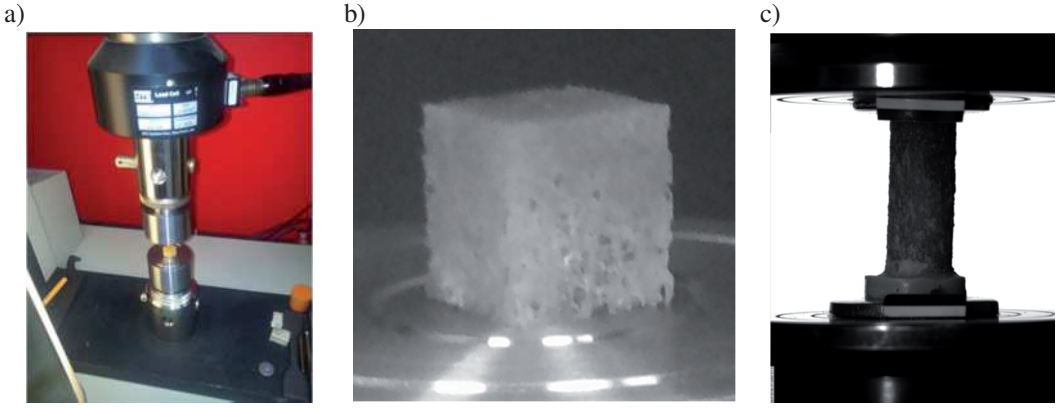

Fig. 4. Compression platens (a), the cubic specimen (b) and cylinder specimen (c)

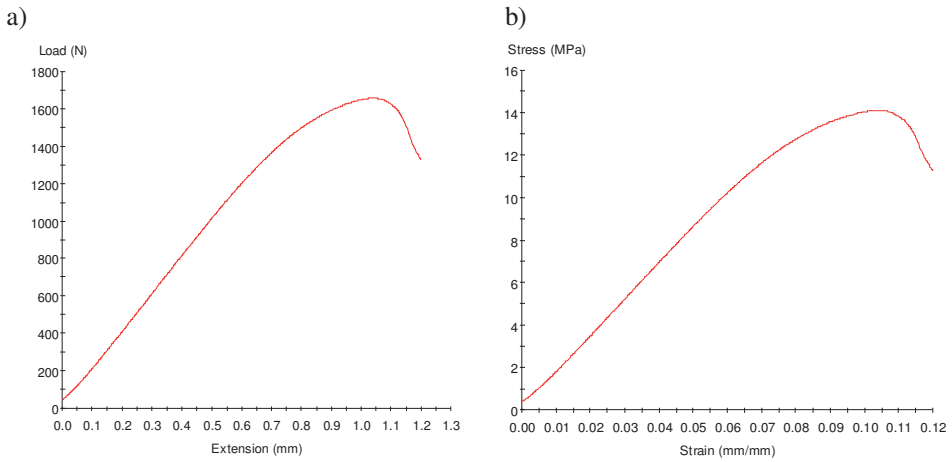

Fig. 5. Typical compression load-extension (a) and stress-strain curve (b) for the spongy bone

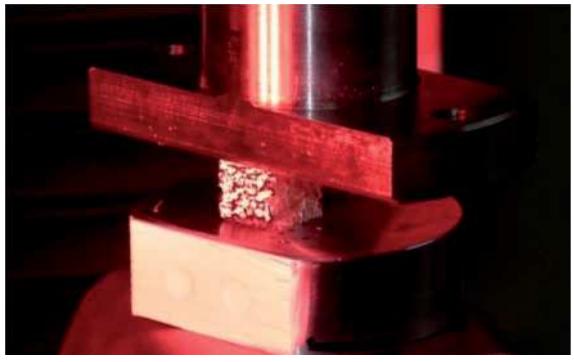

Fig. 6. Testing stand for compression test

The obtained results are repeatable. The diversity of the maximal stress level are connected with the different places where the specimen were taken. It is possible to evaluate the properties directly from the curve, but the results have low accuracy.

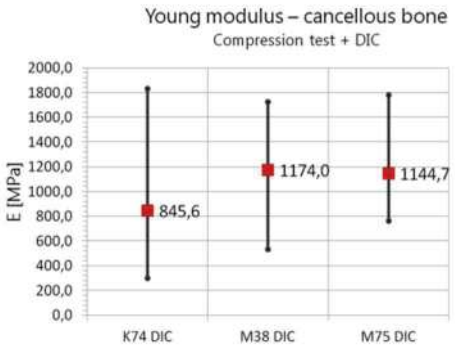

Fig. 7. Young modulus value for the selected samples

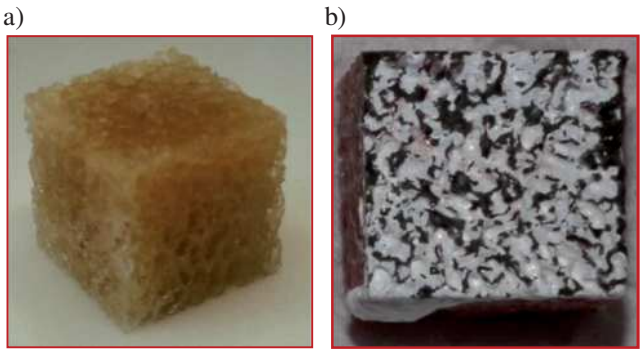

Fig. 8. A sample extracted from a human femur head (a) and with special speckle pattern (b)

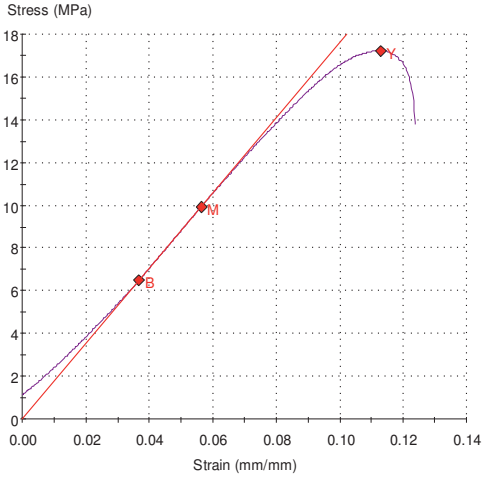

Fig. 9. Selected stress-strain curve for tested samples

As an additional results obtained from the compression test for the cancellous bone wit DIC we can observed displacement field strain field of the tested specimen (Fig. 10).

a) b)

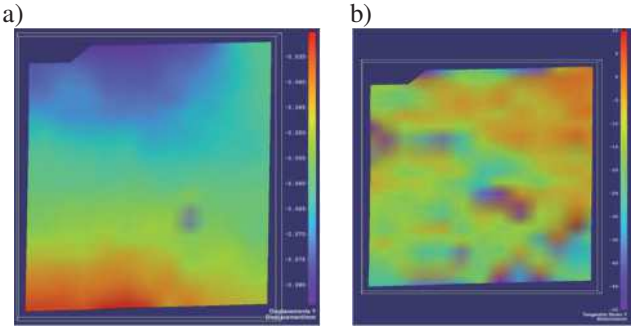

Fig. 10. Displacement field (a) and strain field (b) of the tested specimen

2.3. Three point bending

The second mostly used testing method of the cortical bone is tree or four point bending (Fig. 11). The studies have been performed using human femora dissected from cadaver body from female donor 30 years old. The specimens were dissected from femora diaphysis. The 4x4x40 mm cube shape size of each sample was mechanically machined. Each sample where measure by digital slide caliper (Mitutoyo, resolution 0.01 mm) to control the accuracy of the machining. The method of cutting bone samples and loading method in subsequent tests is shown schematically in Fig.12. Next, according to the DIC procedure, the special spackle pattern was covered the surface of the measured samples (Fig. 13).

a)

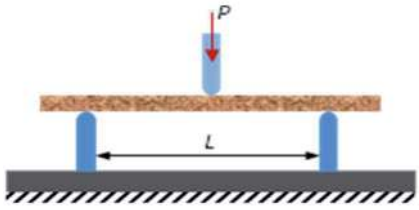

b)

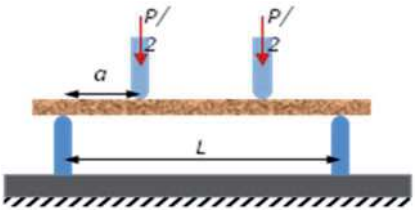

Fig. 11. Scheme of the three point bending (a) and four point bending test (b)

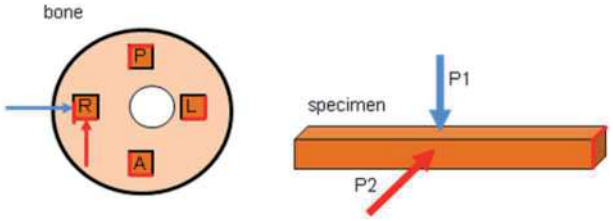

Fig. 12. The method of cutting bone samples and loading in subsequent tests

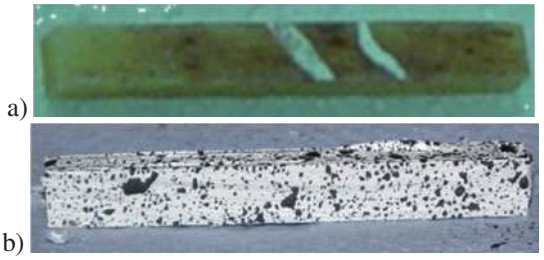

Fig. 13. Prepared sample in the state after the cut (a) and with the special spackle pattern (b)

a)

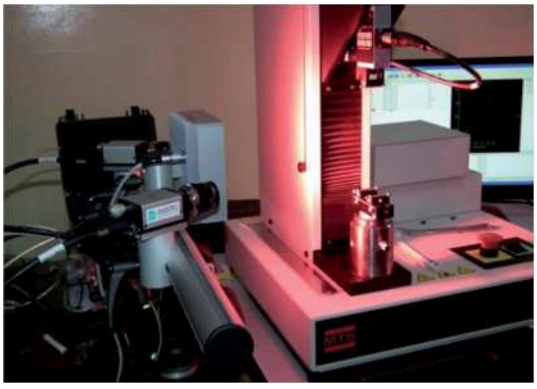

b)

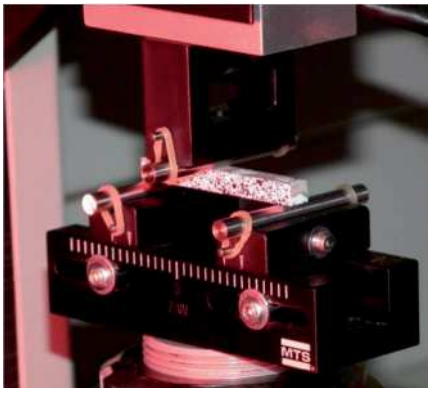

Fig. 14. Three point bending test: a) testing stand with DIC system, b) bending table with the specimen

Based on the curve of load-deflection of the beam and the theory of bending beams the mechanical properties are defined, among others, elastic modulus. For 11 samples obtained an average score of E = 14544 MPa with a standard deviation of 2470 MPa. The testing stand and sample are presented in Fig. 14. Selected load-deflection curve, and also stress-strain curve, shows Fig. 15. Obtained values of Young modulus (with standard deviation) for three samples presented Fig. 16. Using DIC in we additionally obtain coloured displacement map for three point bending (Fig. 17).

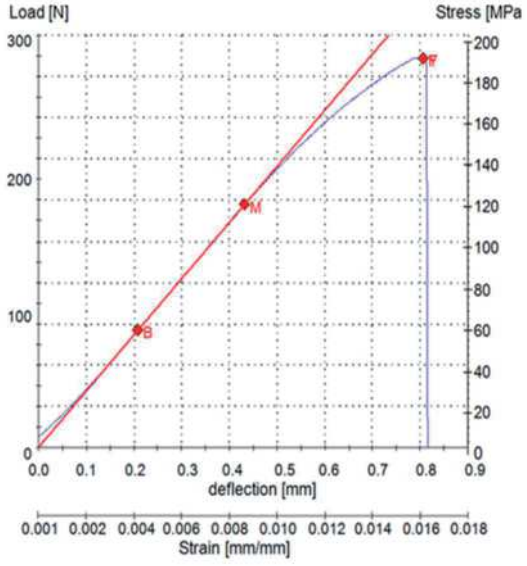

Fig. 15. Selected load-deflection curve, and also stress-strain curve for three point bending

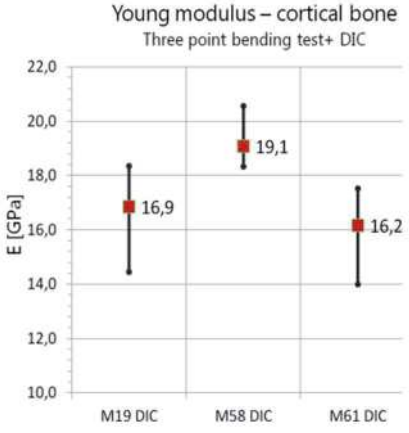

Fig. 16. Young modulus with standard deviation for selected samples

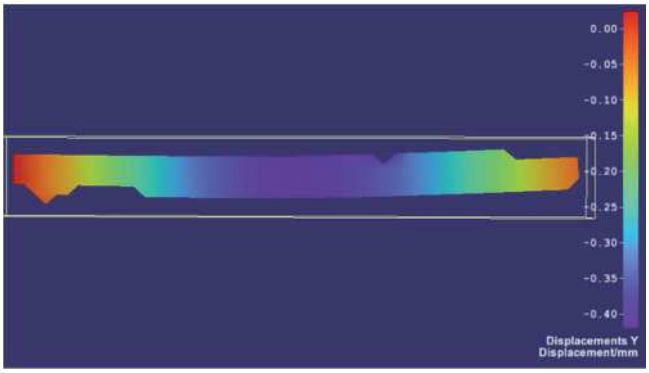

Fig. 17. Colored displacement map from DIC for three point bending

2.4. Nanoindentation

This is relatively new method in the experimental mechanics for testing the hardness and Young modulus. Main advantage is the measurement on the micro- or even nanostructure level. Characteristic for this method is the penetration force range: from mili to microniutons.

The main idea for testing Young modulus is that the penetrator penetrate the sample with the specified force and then sample is controlled unloaded. The first part of unloading curve is connected with ideal elastic behavior of sample. On this basis the Olivier and Pharr developed the method for determining the Young modulus [64]. Tested parameters are calculated directly from the loading-unloading curve (Fig. 18). One can use the following equations to calculate the Young modulus (1) and hardness or micro-hardness (3):

$$E_{IT} = \frac{\left(1-\nu^2\right)}{\frac{1}{E^*_{IT}} - \frac{\left(1-\nu_i^2\right)}{E_i}} \tag{1}$$

$$E^*_{IT} = \frac{\sqrt{\pi}}{2} = \frac{S}{\sqrt{A_p}} \qquad A_p = C_0 h_c^2 + C_1 h_c + C_2 h_c^{1/2} + C_3 h_c^{1/4} + \ldots \tag{2}$$

$$S = \frac{\Delta P_m}{\Delta h_m} \qquad h_c = h_m - \varepsilon \frac{P_m}{S} \ ,$$

$$H_{IT} = \frac{P_m}{A_p} \tag{3}$$

where:
E^*_{IT} – reduced modulus of the indentation contact,
ν – Poisson's ratio of the sample,

ν_i – Poisson's ratio of the indenter (ν_i=0.07),
P_m – loading force,
h_m – penetration depth,
ε – factor dependeing on the diamond shape,
A_p – projected contact area,
C_i – diamond shape dependat.

Figure 19 presents the nanoindentation testing stand.

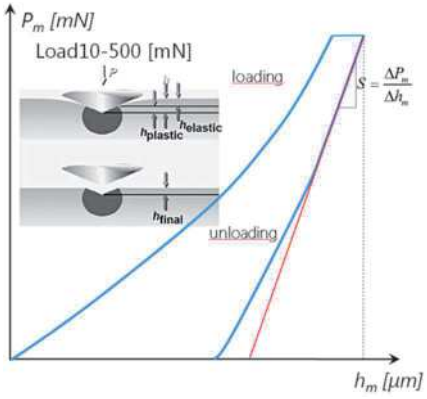

Fig. 18. The nanoindentation curve

a)

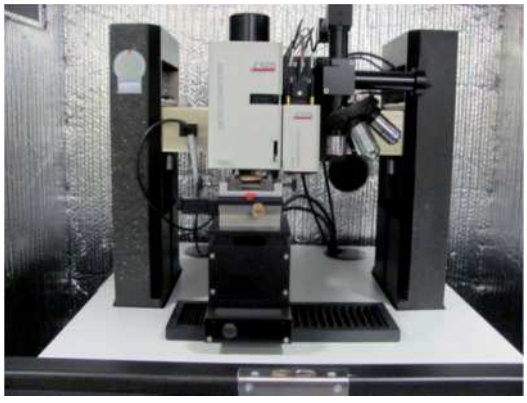

b)

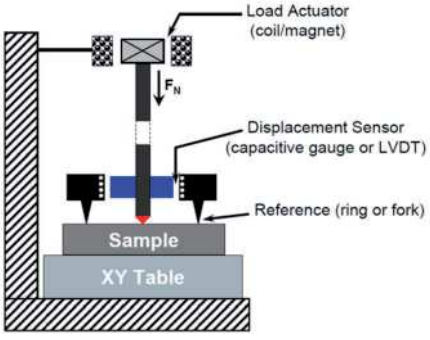

Fig. 19. The nanoindentation testing stand: a) real object (photo), b) schema

Very important in this technique is the proper setup of the testing parameters: load force and times of individual phases. There is not much information in the literature according to tests of the bone tissues using nanoindentation (Bull [65], Ebenstein and Pruitt [36], Fun and Rho [37], Fisher [66], Hoffler et al. [67], Isaksson et al. [68], Lewis and Nyman [69], Menclk and Swain [70], Nemecek [71], Norman et al. [24], Rho and Pharr [72], Rho et al. [73], Rodriguez-Florenza et al. [74], Swadener et al. [75], Wu et al. [76], Zysset et al. [77]) but we can find many results. Those which had been found gave wrong results. For this reason we performed additional tests for evaluating our own values for loading force and phase times. On the basis of the conducted research we determine the loading force range which is 200-600 mN both for cancellous and cortical bone.

The influence of the force value on the results are presented in Fig. 20. It can be observed that values higher than 100 mN secure the repeatability of results.

a)

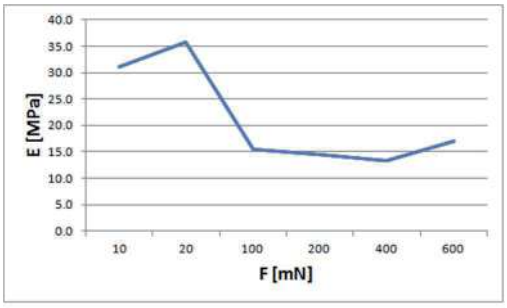

b)

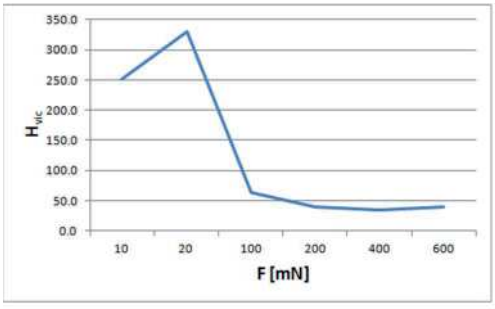

Fig. 20. Setup of the penetration force value: Young modulus – load force (a), hardness H_{VIC} – load force (b)

The nanoindentation was used for evaluation of the Young modulus and micro-hardness both for the cancellous and cortical bone. In the Fig. 21 the characteristic parts of the tarabecular structure are presented – single trabecula and nodes. Series of tests for single trabecula and for single nodes were performed and the

differences in the results Have been observed. In the specified places the Young modulus and microhardness were evaluated.

On the base of the conducted series of tests for single trabecula the Young modulus vary between 8.4-13.3 GPa, the Vickers micro-hardness vary between 50.1-55.9 (Table 1, avg. value). The example of testing the cortical bone is presented in the Fig. 22. We can see testing stand, samples and microscopic view of the tested places.

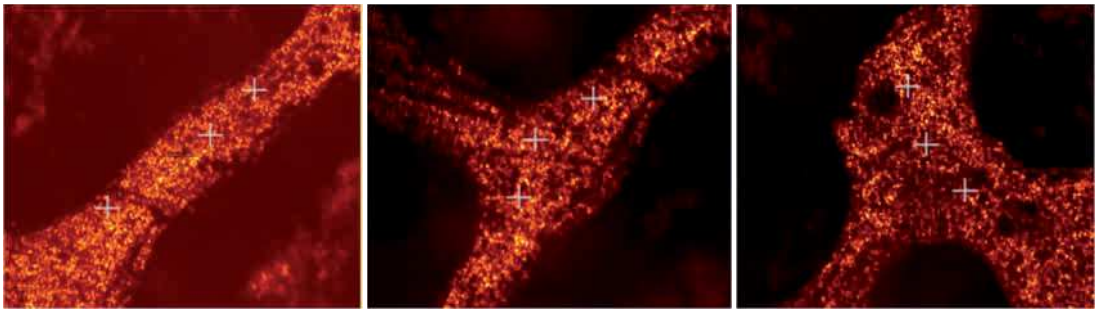

trabecula node I node II

Fig. 21. Single trabecula and nodes under microscope with measurement points

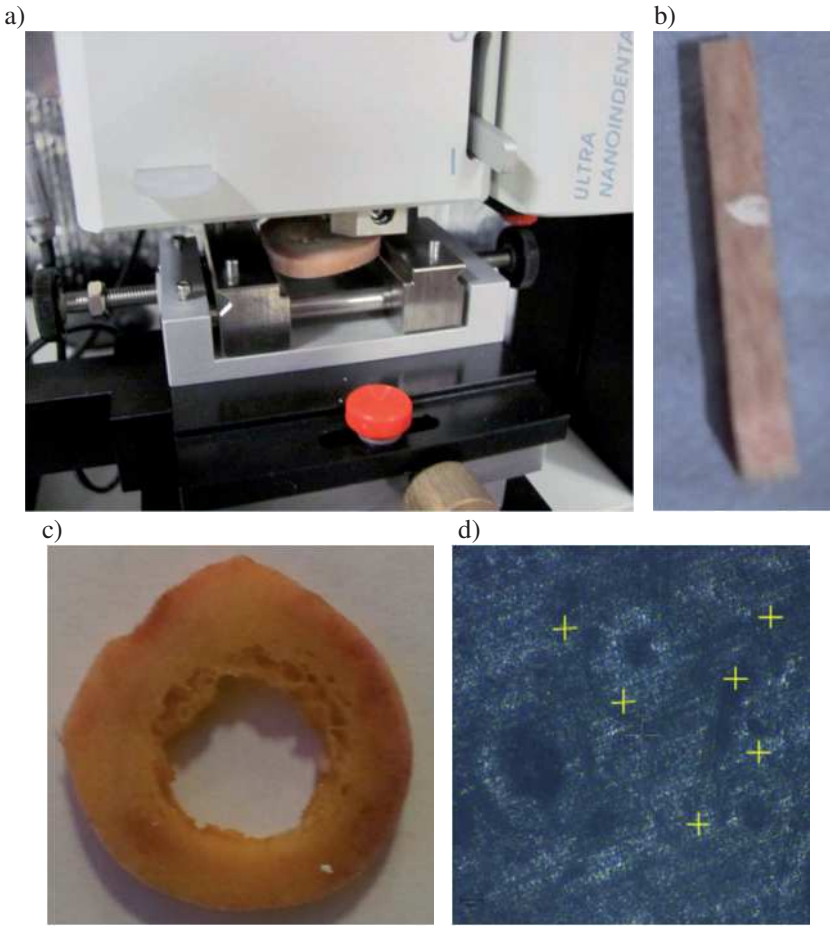

Fig. 22. Nanoindentation: a) testing stand, b), c) samples, d) microscopic view of the tested places

Table 1.
Results of nanoindentation test of trabecular bone tissue

	test	F	E	H_{IT}	H_{VIC}
		mN	GPa	MPa	Vickers
Trabeculae	1	200	8.494	500.3	47.2
	2	200	8.424	564.5	53.3
	3	200	8.299	545.8	51.5
	avg.		8.4	536.9	50.7
	1	200	9.854	592.0	55.8
Node I	2	200	10.324	542.0	54.4
	3	200	9.954	584.0	57.6
	avg.		10.0	572.7	55.9
	1	200	13.664	514.3	48.5
Node II	2	200	13.666	593.0	55.9
	3	200	12.635	485.5	45.8
	avg.		13.3	530.9	50.1

3. Numerical simulation

3.1. Identification of the material parameters using evolutionary optimization system

There is also possibility of evaluation the mechanical properties using the numerical simulation. Here, the identification process using the evolutionary methods and finite element method is prescribed.

Because we want to know material properties, we must define identification problem. In fact, the inverse problem should be solved. The identification problem is to find material coefficients such as Young modulus and Poisson's ratio. The vector of design variables x, which contains design variables, corresponds to material properties. The material coefficients can be found by minimizing a functional formulated as differences between measured displacements (using DIC) and displacements obtained using numerical simulation (Eq. 4). The evolutionary algorithm operates on populations of individuals. The individual consist of chromosomes. The individual is often called chromosome if consist of one chromosome. Each chromosome contains genes. Genes contain information about design variables values. The fitness function value which plays the role of optimization functional is computed for every chromosome in population. First starting population is created randomly. Then the fitness function value for each chromosome is evaluated. Next evolutionary operators changes genes values in some chromosomes. The offspring population is created as a result of a selection process. The next iteration is performed if the stop criterion is not fulfilled. The stop criterion can be formulated as maximum number of iterations or stop after achieving the predefined fitness function value.

$$\begin{aligned} &min \quad F(\boldsymbol{x}) = \left| u_{y\,exp} - u_y(\boldsymbol{x}) \right| \\ &\boldsymbol{x} = [E_{TRAB}, \nu_{TRAB}] \end{aligned} \tag{4}$$

Here, all specimens were scanned using the micro tomography. On the base of obtained slides using the specialized software from MIMICS Materialize the smooth discrete models were prepared (Fig. 23).

In order to identify cancellous bone material parameters the optimization problem has been define. The objective function was built on the base of displacement obtained from the compression test wit DIC (Eq. 4). The constrains are connected with young modulus and trabecula Poisson coefficient (Eq. 5). The used evolutionary algorithm parameters are presented in the Table 2. The schema of evolutionary optimization system shows Fig. 24.

$$\begin{aligned} 500MPa < E_{TRAB} < 1500MPa \\ 0.2 < \nu_{TRAB} < 0.4 \end{aligned} \tag{5}$$

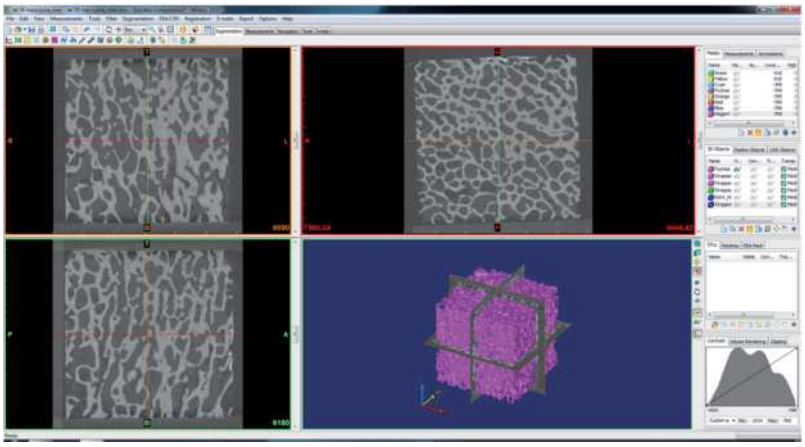

Fig. 23. Model preparation using MIMICS materialize

Table 2.
Evolutionary algorithm parameters

Parameter	Value
Subpopulation number	2
Number of cromosoms in population	10
Probability of Gauss mutation	0.9
Probability of mutation	0.1
Number of iteration	20

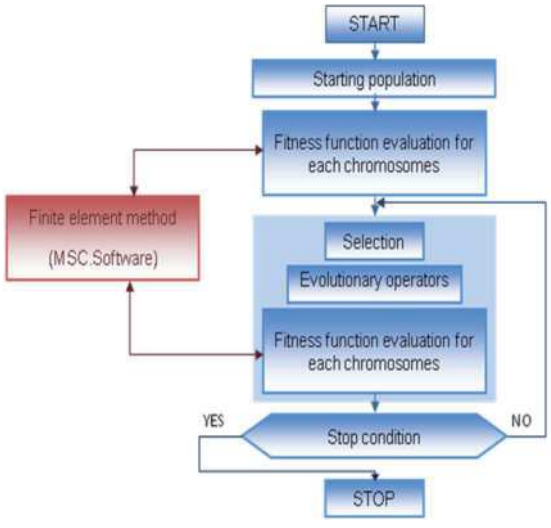

Fig. 24. The schema of evolutionary optimization system

Obtained results are close to the results from nanoindentation (Fig. 25, Tab. 3). Also the displacement field of the numerical model with indentified parameters are close to the experimental one with the use of the digital image correlation (Fig. 26).

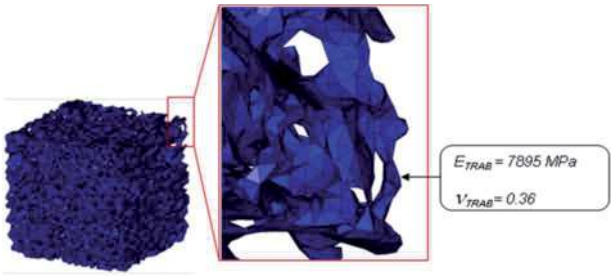

Fig. 25. Numerical model with identified material parameters for individual trabecula

Table 3.
Material parameters from identification and nanoindentation

Parameter	Identification	Nanoindentation
Young modulus E, MPa	7895	8405
Poisson ratio ν	0.36	0.34

a) b)

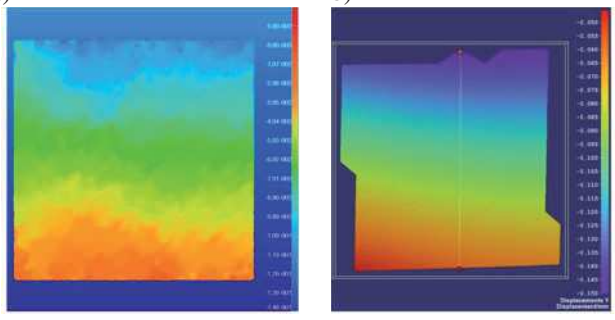

Fig. 26. Displacement field form numerical simulation (a) and experiment (b) for identify material parameters

3.2. Three point bending test simulation

For the one specimen with Young modulus E≅22200 MPa and ultimate tensile strength S=319 MPa with max. deflection y=0.69 mm the numerical simulation was performed. The sample was scanned by X-ray microcomputed tomography (XMT) scanner (Nikon Metrology, X-tek, Tring, UK). Scanning settings (kV, μA, no filter, 2000 projections, voxel size 20 μm) were adjusted using the manufacturer software. The density phantom was scanned together with the specimen to enable quantitative measurement of the bone mineral density. After image acquisition reconstruction of cross-sectional axial images were performed. The total volume of interest contains 2000x2000x2000 voxels from about 356 000 voxels were busy with the bone friction. The reconstructed volume was stored in the single file (32-bits real, little endian) on the computer hard drive.

The FE model with material parameters was generated automatically, based on approach described by [11,25] and own developed software. For each voxel contained bone one element (HEXA 8-noded) was defined. Based on calibrated grey value material parameters (Young modulus E, ultimate strength S) have been defined. Relationship which connects calibrated bone density with material properties were defined based on following equations:

$$E = 10.5 + 0.0102\rho_{QCT}; \quad (6)$$

$$S = 63.8 + 0.184\rho_{QCT} \quad (7)$$

where ρ_{QCT} – density calibrated based on greyscale and calibration curve.

This gives the model with non-homogenous material parameters what is closer to the reality then taking into account the model with one material with linear properties. The FE model was built using the HEXA 8-noded elements and consist of about 3 mln DOF. Specimen with material parameters is presented in Fig 27a. Boundary condition were taken from the experiment and modelled in the MSC.Patran (Fig. 27b). Simulation were performed using the MSC.Nastran solver. The finite element analysis gives the results presented in Fig. 28. The max. normal stress is $\sigma x \cong 314$ MPa and deflection y≅0.73 mm The results from simulation matched the results from the experiment (Fig. 17).

The numerical calculations using finite element method give the deflection and stresses comparable with experimental results. It shows that the numerical analysis of models generated on the base of X-ray microcomputed tomography (XMT) scans with material parameters described based on Hounsfiled scale can be used as the tool for determining the mechanical properties of bone. The computational methods primary used in mechanics can be useful for solving the biomechanics problems too.

a)

b)

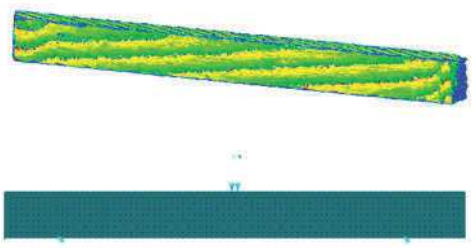

Fig. 27. The specimen FE: a) model generated from XMT with assigned materials properties, b) FE model with boundary conditions

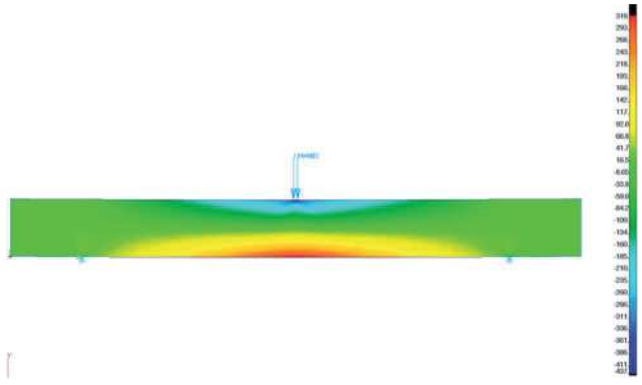

Fig. 28. The stress distribution in specimen

3.3. Numerical analysis and experimental verification of human femur for selected gait phase load

The pelvic joint before reconstruction – in anatomically shape, was tested to obtain the data for comparison the strain and the stress state in trabecular and cortical bone tissues (in femur) before and after reconstruction. The results were obtained in two ways: from experiment and numerical simulation.

In the experiment MTS Insigth testing machines and DIC, as the displacement and strain measurement system were used. During the test preparation there were occurred some problems which were solved successfully:

- a special system for fix the sample was proposed,
- a cyclic load applied to sample (femur head) was programmed,
- a stochastic pattern on the bone sample surface was plotted,
- system was calibrated and selected data were recorded.

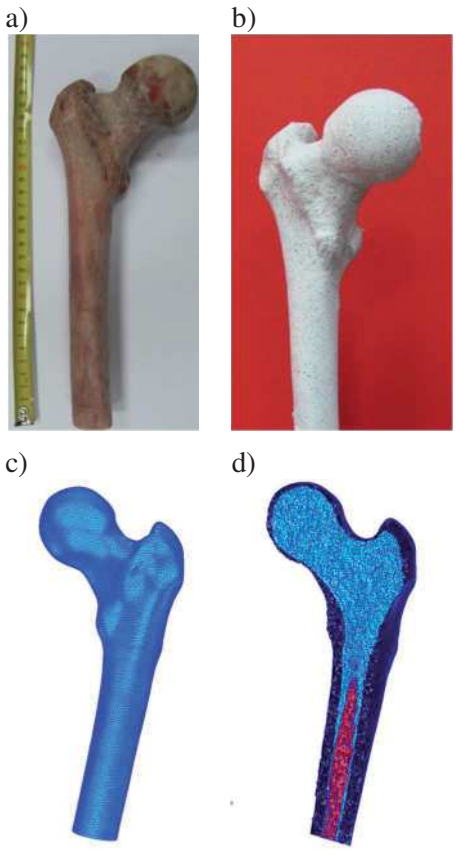

Fig. 29. The tested femur (a), stochastic pattern on the bone specimen (b), numerical model with FEM mesh (c), material distribution in the cross-section (d)

The tested femur in initial form and with stochastic pattern on external surface show Fig. 29a and Fig. 29b. Figure 29c presents numerical model with FEM mesh and Fig. 29d presents material distribution in the cross-section of prepared model of the femur. The test stand with tested sample shows Fig. 30. An example of cyclic load diagram applied to sample shows Fig. 31 and respectively an example of displacement diagram shows Fig. 32.

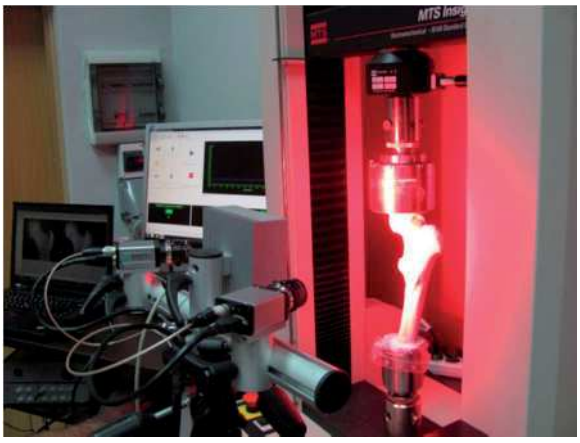

Fig. 30. Test stand with MTS testing machine and DIC system

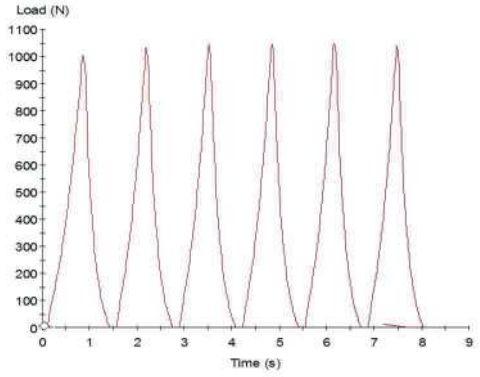

Fig. 31. Selected example of load diagram

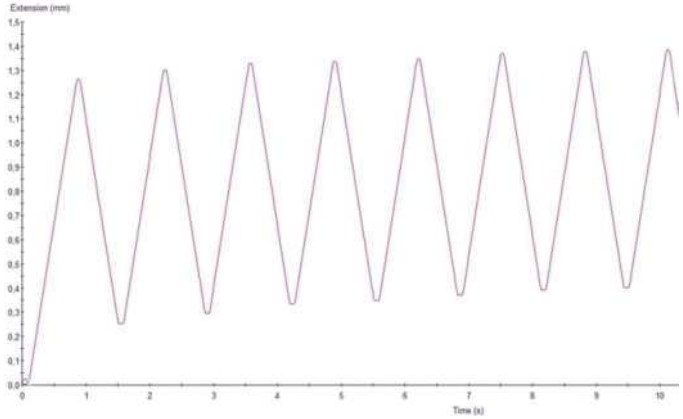

Fig. 32. An example of displacement diagram

As the results from DIC the strain diagrams and the displacement maps were observed (Fig. 33 and Fig. 34).

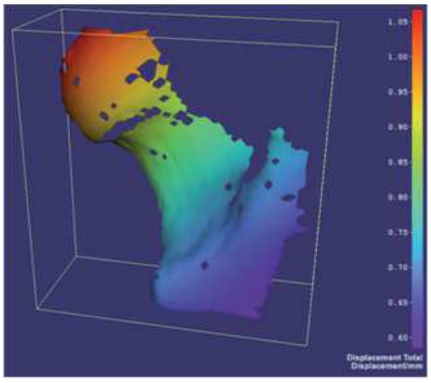

Fig. 33. The strain diagram from DIC

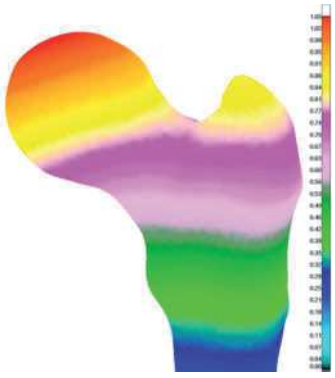

Fig. 34. The displacement maps from DIC

The model of bone specimens was created on the basis of CT scans, took with high accuracy (0.347 mm). After building and assembling the CAD model was divided into high value of finite elements. Preparing of the finite element model was the most time consuming stage. The next step it was to assign material data to each element. The special equations were used at this step (Rho et al. [11,25]). The equations for cancellous bone of femur sometimes described material characteristic for pelvis due to lack of appropriate data. The final results are shown in Table 4.

The analysis was done in MSC.Marc. Boundary conditions mimicked the real experiment. The femur was reoriented and fixed in bottom part of shaft for this reason.

The values of force were established on three different values, which first (600 N) was in accordance with the experiment (Load 1). Two last vales corresponded to the multiplication of the body weight (BW=85 kg). The second (Load 2) was the 238% of BW (the value of hip joint reaction during full stand phase) and the last (Load 3) was 600% of BW (the reaction during the landing phase of jump up).

The tasks were solved in elastic range. The Coulomb bilinear model of contact was used for modelling the touching of cement part to the femoral head. The coefficient of friction was established on 0.2. The number of DOF was 157 140 and the time of computation was the 1285 s.

Results obtained for applied load show Figures 35-37.

The comparison of results obtained from analysis of femur loaded by 600N with results from DIC experiment indicates a good agreement between them. There could be noted that principal maximal as well minimal strain of cortex obtained from FEM analysis are generally in range <-0.002;0.002>. In case of the DIC experiment, almost the whole examined surface of cortex is in this same range, except the point values which exceed the range from top or bottom.

The FEM analysis allowed to observe the stress as well strain distribution in case of trabecular bone in different load cases. Generally, the areas of distribution are the same due to exact these same direction of loads.

Table 4.
Material parameters in FE model

	Realation	Apparent density, ρ_{app}	Young modulus, E	Poisson coef. ν
Marrow	----------	----------	1 MPa	0.3
Trabecular bone	$\rho_{app}=0.67(131+1.067HU)$ $E=0.658(0.00390\rho_{app}^{1.96})$	500 kg/m^3	<661HU: 365 MPa Total: 500 MPa	0.4
Cortical bone	$\rho_{app} = 0.79(0.769HU+1028)$ $E=0.807(14\rho_{app}-6142)$	1500 kg/m^3	12 GPa	0.33

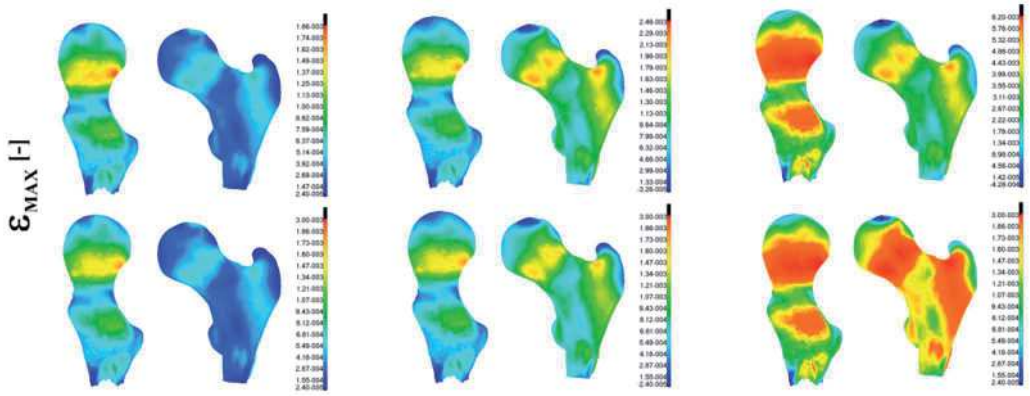

Fig. 35. Trabecular bone-strain distribution

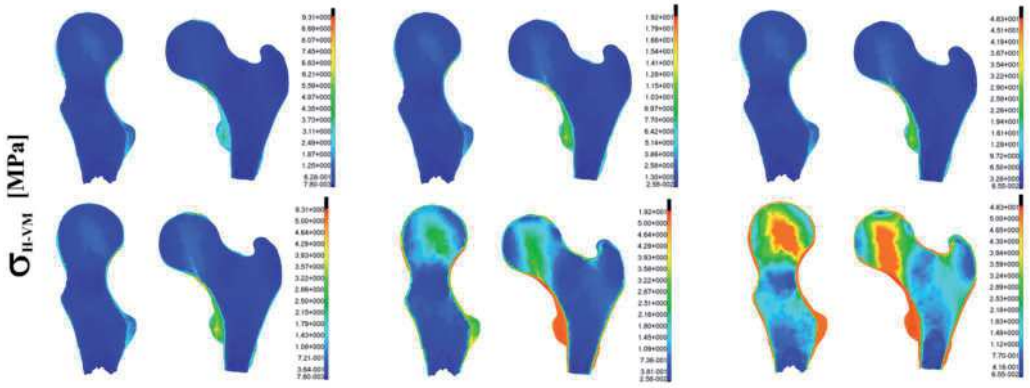

Fig. 36. Trabecular bone-stress distribution

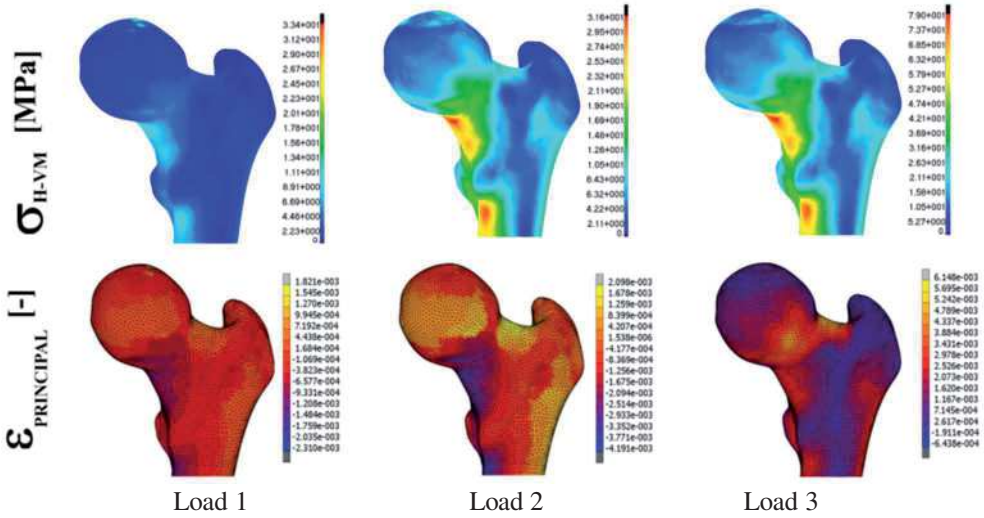

Fig. 37. Cortical bone-stress and strain distribution

The difference occurs in the case of values. The main finding which could be pointed, is that for 238%BW, the values of reduced stress in accordance with the Huber-von Misses hypothesis as well as principal values of strain do not exceed the yield stress and strain (σ_y=4.89±3.77 MPa; $\varepsilon_{y\_tension}$=0.0063±0.0005; $\varepsilon_{y\_compression}$=0.0101±0.0018).

The higher distribution of stresses occurs in femoral neck area not inside, but outside the bone. In this area the trabecular bone has the high values of Young modulus *E*, so also the yield stress is quite high (σ_y=15.29±4.87 MPa).

In case of the 600%BW of loading force the highest values concentration of stresses is in the same area, but the values exceed the σ_y. This area is in the place of transferring the load into cortex of femoral shaft. In this particular area the maximal reduced stress is 79 MPa, while the σ_y=133.4 MPa

4. Conclusions

Combination of numerical simulation and experimental research is needed to obtain correct results and broaden the spectrum of relevant parameters necessary to support surgical and rehabilitation. Both approaches require modern equipment and advanced testing methods. Based on the survey conclusions can be formulated as follows.

Advanced methods allow to measure the displacement and strain on biological specimens. Here, the MTS universal testing machine (MTS Insigth 10 kN) connected with the Digital Image Correlation system (Dantec Dynamics) were used.

Obtained results allow to compare the displacement and strain from experiment and numerical simulation. The comparison indicates a good agreement between them.

Generally, in experiment we can observed selected results (displacement and strain using DIC) on the external surface of sample. On the base of displacement and strain we can calculate the stresses after assuming material parameters. From numerical simulation, after FEM analysis we obtained full set of mechanical parameters useful in planning of surgical intervention (THA, pelvis reconstruction), aided the diagnostic in risky state and design of prosthesis.

Only the numerical model verified in experiment can be used in computer aided of medical interventions. In this work numerical models were verified and obtained results may provide a basis for future research.

References

[1] S.C. Cowin (Ed.), Bone mechanics handbook, CRC Press LLC, 2001.

[2] Y.H. An, R.A. Draughn, Mechanical testing of bone and the bone–implant interface, CRC Press, Boca Raton, USA, 2000.

[3] T.M. Keaveny, E.F. Morgan, O.C. Yeh, Bone mechanics, in: Standard handbook of biomedical engineering and design, The McGraw-Hill Co., 2004.

[4] R.B. Ashman, J.Y. Rho, Elastic modulus of trabecular bone material, Journal of Biomechanics 21 (1988) 77-81.

[5] S. Boutroy, B. van Rietbergen, E. Sornay-Rendu, F. Munoz, M.L. Bouxsein, P.D. Delmas, Finite element analysis based on in vivo HR-pQCT images of the distal radius is associated with wrist fracture in postmenopausal women, Journal of Bone and Mineral Research 23/3 (2008) 393-399.

[6] B. Helgason, E. Perilli, E. Schileo, F. Taddei, S. Brynjólfsson, M. Viceconti, Mathematical relationships between bone density and mechanical properties: A literature review, Clinical Biomechanics 23 (2008) 135-146.

[7] R. Hodgskinson, J.D. Currey, Young's modulus, density and material properties in cancellous bone over a large density range, Journal of Material Science: Materials in Medicine 3 (1992) 377-381.

[8] J.H. Keyak, I.Y. Lee, H.B. Skinner, Correlations between orthogonal mechanical properties and density of trabecular bone: use of different densitometric measures, Journal of Biomedical Material Research 28 (1994) 1329-1336.

[9] J.H. Keyak, T.S. Kaneko, J. Tehranzadeh, H.B. Skinner, Predicting proximal femoral strength using structural engineering models, Clinical Orthopaedics and Related Research 437 (2005) 219-228.

[10] W. Pistoia, B. van Rietbergen, F. Eckstein, C. Lill, E.M. Lochmuller, P. Rüegsegger, Prediction of Distal Radius Failure with μFE Models Based on 3D-PQCT Scans, Advances in Experimental Medicine and Biology 496 (2001) 143-151.

[11] J.Y. Rho, M.C. Hobatho, R.B. Ashman, Relations of mechanical properties to density and CT number in human bone, Medical Engineering and Physics 17 (1995) 347-355.

[12] L. Feng, I. Jasiuk, Effect of specimen geometry on tensile strength of cortical bone, Journal of Biomedical Materials Research A 95/2 (2010) 580-587.

[13] K.B. Garnier, R. Dumas, C. Rumelhart, M.E. Arlot, Mechanical characterization in shear of human femoral cancellous bone: torsion and shear tests, Medical Engineering and Physics 21 (1999) 641-649.

[14] T.M. Keaveny, R.E. Borchers, L.J. Gibson, W.C. Hayes, Theoretical analysis of the experimental

artifact in trabecular bone compressive modulus, Journal of Biomechanics 26/4-5 (1993) 599-607 http://dx.doi.org/10.1016/0021-9290(93)90021-6.
[15] T.M. Keaveny, T.P. Pinilla, R.P. Crawford, D.L. Kopperdahl, A. Lou, Systematic and random errors in compression testing of trabecular bone, Journal of Orthopeadic Research 15/1 (1997) 101-110.
[16] T.S. Keller, Predicting the compressive mechanical behavior of bone, Journal of Biomechanics 27 (1994) 1159-1168.
[17] A. Öchsner, W. Ahmed, Biomechanics of hard tissues. Modeling, testing and materials, Wiley-VCH Verlag GmBH&Co. KGaA, Weinheim, 2010.
[18] D.T. Reilly, A.H. Burstein, The elastic and ultimate properties of compact bone tissue, Journal of Biomechanics, 8 (1975) 393-405.
[19] A. Sanyal, A. Gupta, H.H. Bayraktar, R.Y. Kwon, T.M. Keaveny, Shear strength behavior of human trabecular bone, Journal of Biomechanics 45 (2012) 2513-2519.
[20] M. Kasra, M.D. Grynpas, On shear properties of trabecular bone under torsional loading: Effects of bone marrow and strain rate, Journal of Biomechanics 40 (2007) 2898-2903.
[21] E. Hamed, I. Jasiuk, A. Yoo, Y.H. Lee, T. Liszka, Multi-scale modelling of elastic moduli of trabecular bone, Journal of the Royal Society Interface 9/72 (2012) 1-20.
[22] T.M. Keaveny, O.C. Yeh, Architecture and trabecular bone – toward an improved understanding of the biomechanical effects of age, sex and osteoporosis, Journal of Musculoskeletal and Neuron Interact 2/3 (2002) 205-208.
[23] P. Makowski, A. John, W. Kuś, G. Kokot, Multiscale modeling of the simplified trabecular bone structure, Proceedings of the 18th International Conference: Mechanics, Kaunas, 2013, 136-161.
[24] J. Norman, J.G. Shapter, K. Short, L.J. Smith, N.L. Fazzalari, Micromechanical properties of human trabecular bone: A hierarchical investigation using nanoindentation, Journal of Biomedical Materials Research A 87/1 (2008) 196-202.
[25] J.Y. Rho, L. Kuhn-Spearing, P. Zioupos, Mechanical properties and the hierarhical structure of bone, Medical Engineering and Physics 20 (1998) 92-102.
[26] B. van Rietbergen, Micro-FE analyses of bone: state of the art, in: Noninvasive Assessment of Trabecular Bone Architecture and the Competence of Bone, S. Majumdar, B.K. Bay (Eds.), Chapter: Metrics, Vol. 496: Advances in Experimental Medicine and Biology, Springer, 2001, 21-30.
[27] T.J. Vaughan, C.T. McCarthy, L.M. McNamara, A three-scale finite element investigation into the effects of tissue mineralisation and lamellar organisation in human cortical and trabecular bone, Journal of the Mechanical Behavior of Biomedical Materials 12 (2012) 50-62.
[28] H. Wang, B. Ji, S. Liu, E. Guo, Y. Huang, K.C. Hwang, Analysis of microstructural and mechanical alterations of trabecular bone in a simulated three-dimensional remodeling process, Journal of Biomechanics 45 (2012) 2417-2425.
[29] X. Wang, J.S. Nyman, X. Dong, H. Leng, M. Reyes, Fundamental Biomechanics in Bone Tissue Engineering, Morgan & Claypool, 2010.
[30] M. Binkowski, G.R. Davis, Z. Wróbel, A.E. Goodship, Quantitative Measurement of the Bone Density by X-Ray Micro Computed Tomography, C.T. Lim, J.C.H. Goh (Eds.), WCB 2010, IFMBE Proceedings Vol. 31, 2010, 856-859.
[31] M. Binkowski, A. Dyszkiewicz, Z. Wróbel, The analysis of densitometry image of bone tissue based on computer simulation of X-ray radiation propagation through plate model, Computers in Biology and Medicine 37/2 (2006) 245-250.
[32] M. Binkowski, E. Tanck, M. Barink, W.J. Oyen, Z. Wróbel, N. Verdonschot, Densitometry test of bone tissue: Validation of computer simulation studies, Computational Biological Medicine 38/7 (2008) 755-764.
[33] Ł. Cyganik, M. Binkowski, G. Kokot, T. Rusin, P. Popik, F. Bolechała, R. Nowak, Z. Wróbel, A. John, Experimental verification of the relationships between Young's modulus and bone density using digital image correlation, Proceedings of the PCM-CMM-2015 Congress, CRC Press/Balkema, 2016, 133-136.
[34] Ł. Cyganik, M. Binkowski, G. Kokot, T. Rusin, P. Popik, F. Bolechała, R. Nowak, Z. Wróbel, A. John, Prediction of Young's modulus of trabeculae in microscale using macro-scale's relationships between bone density and mechanical properties, Journal of the Mechanical Behavior of Biomedical Materials 36 (2014) 120-134, doi: 10.1016/j.jmbbm.2014.04.011.
[35] D. Christen, A. Levchuk, S.A. Schor, P. Schneider, S.K. Boyd, A. Müller, Deformable image registration and 3D strain mapping for the quantitative assessment of cortical bone microdamage, Journal of the Mechanical Behavior of Biomedical Materials 8 (2012) 184-193.
[36] D.M. Ebenstein, L.A. Pruitt, Nanoindentation of biological materials, NanoToday 1/3 (2006) 26-33.

[37] Z. Fan, J.Y. Rho, Effects of viscoelasticity and time-dependent plasticity on nanoindentation measurements of human cortical bone, Journal of Biomedical Materials Research A 67/1 (2003) 208-214.
[38] K. Janca, J. Tarasiuk, A.S. Bonnet, P. Lipinski, Genetic algorithms as a useful tool for trabecular and cortical bone segmentation, Computer Methods and Programs in Biomedicine 111/1 (2013) 72-83 http://dx.doi.org/10.1016/j.cmpb.2013.03.012.
[39] A. John, G. Kokot, Experimental testing and numerical simulation of bone tissue, Annals of Faculty Engineering Hunedoara – International Journal of Engineering 14/3 (2016) 55-66.
[40] A. John, G. Kokot, The test of implementation the orthotropic material properties in numerical model of human pelvic bone, Proceedings of the 1st Conference "Computational Mechanics" CEACM and Proceedings of the 15th International Conference "Computer Methods in Mechanics" CMM2003, Gliwice-Wisła, 2003, 161-162 (on CD).
[41] A. John, G. Kokot, The anisotropic material properties in numerical model of the human pelvic bone, Proceedings of the International Conference "Numerical Methods in Continuum Mechanics" NMCM2003, Extended Abstracts, Zilina, 2003, 55-56.
[42] A. John, W. Kuś, The identification of material coefficients of human pelvic bone using evolutionary algorithm, Proceedings of AI-METH 2002, Gliwice, 2002, 201-204.
[43] A. John, W. Kuś, P. Orantek, Material coefficients identification of bone tissues using evolutionary algorithms, M. Tanaka (Ed.), Inverse Problems in Engineering Mechanics IV, Elsevier, 2003, 95-102.
[44] G. Kokot, M. Binkowski, A. John, B. Gzik-Zroska, Advanced mechanical testing methods in determining bone material, Proceedings of the 17th International Conference "Mechanics", Kaunas, 2012, 139-143.
[45] A. John, M. Duda, G. Kokot, The analysis of femur and parametric endoprosthesis system, Proceedings of the 17th International Conference "Mechanics", Kaunas, 2012, 99-105.
[46] R. Rezende, M. Rezende, P. Bártolo, A. Mendes, R.M. Filho, Optimization of Scaffolds in Alginate for Biofabrication by Genetic Algorithms, Computer Aided Chemical Engineering 27 (2009) 1935-1940.
[47] B. van Rietbergen, S. Majumdar, W. Pistoia, D.C. Newitt, M. Kothari, A. Laib, P. Rüegsegger, Assessment of cancellous bone mechanical properties from micro-FE models based on micro-CT, μQCT and MR images, Technology and Health Care 6 (1998) 413-420.
[48] N. Vilayphiou, S. Boutroy, E. Sornay-Rendu, B. van Rietbergen, F. Munoz, P.D. Delmas, R. Chapurlat, Finite element analysis performed on radius and tibia HR-pQCT images and fragility fractures at all sites in postmenopausal women, Bone 46 (2012) 1030-1037.
[49] H. Beaupied, E. Lespessailles, C.L. Benhamou, Evaluation of macrostructural bone biomechanics, Joint Bone Spine 74 (2007) 233-239.
[50] I.G. Jang, I.Y. Kim, Computational simulation of simultaneous cortical and trabecular bone change in human proximal femur during bone remodeling, Journal of Biomechanics 43 (2012) 294-301.
[51] T.H. Lim, J.H. Hong, Poroelastic properties of bovine vertebral trabecular bone, Journal of Orthopaedic Research 18 (2000) 671-677.
[52] L.P. Mullins, M.S. Bruzzia, P.E. McHugh, Measurement of the microstructural fracture toughness of cortical bone using indentation fracture, Journal of Biomechanics 40 (2007) 3285-3288.
[53] A. Nazarian, D. von Stechow, D. Zurakowski, R. Muller, B.D. Snyder, Bone Volume Fraction Explains the Variation in Strength and Stiffness of Cancellous Bone Affected by Metastatic Cancer and Osteoporosis, Calcified Tissue International 83 (2008) 368-379.
[54] G.L. Niebur, T.M. Keaveny, Computational modeling of trabecular bone, in: Computational Modeling in Biomechanics, Suvranu De, Farshid Guilak, Mohammad Mofrad R.K. (Eds.), Chapter, Springer, 2009, 277-306.
[55] C. Oomens, M. Brekelmans, F. Baaljens, Biomechanics. Concepts and computations, Cambridge University Press, Cambridge, 2009.
[56] W.M Saltzman, Biomedical engineering, Bridging Medicine and Technology, Cambridge University Press, 2009.
[57] E. Tanck, J.B. van Aken, Y.M. van der Linden, H.W. Bart Schreuder, M. Binkowski, H. Huizenga, N. Verdonschot, Pathological fracture prediction in patients with metastatic lesions can be improved with quantitative computed tomography based computer models, Bone 45 (2009) 777-783.
[58] E. Verhulp, Analyses of trabecular bone failure, Universiteitsdrukkerij TU Eindhoven, Eindhoven, The Netherlands, 2006.
[59] D.C. Writz, N. Schiffers, T. Pandorf, K. Radermacher, D. Weichert, R. Forst, Critical evaluation of known bone material properties to realize anisotropic FE-simulation of the proximal femur, Journal of Biomaterials 33 (2000) 1325-1330.
[60] Application Note, T-Q-400-Basics-3DCORR-002a-EN, Basics of 3D Digital Image Correlation, Dantec Dynamics.

[61] Technical Note, T-Q-400-Accuracy-3DCORR-003-EN, Error Estimations of 3D Digital Image Correlation Measurements, Dantec Dynamics.
[62] P. Sztefek, M. Vanleene, R. Olsson, R. Collinson, A.A. Pitsillides, S. Shefelbine, Using digital image correlation to determine bone surface strains during loading and after adaptation of the mouse tibia, Journal of Biomechanics 43 (2010) 599-605.
[63] E. Verhulp, B. van Rietbergen, R. Huiskes, A three-dimensional digital image correlation technique for strain measurements in microstructures, Journal of Biomechanics 37 (2004) 1313-1320.
[64] W.C. Olivier, G.M. Pharr, An improved technique for determining hardness and elastic-modulus using load and displacement sensing indentation experiments, Journal of Materials Research 7/6 (1992) 1564-1583.
[65] S. Bull, Extracting hardness and Young's modulus from load-displacement curves, Zeitschrift für Metallkunde 93/9 (2002) 870-874.
[66] A.C. Fischer Cripps, The IBIS Handbook of Nano-indentation, Fischer Crips Laboratories Pty Ltd., 2009.
[67] C.E. Hoffler, X.E. Guo, P.K. Zysset, S.A. Goldstein, An application of nanoindentation technique to measure bone tissue Lamellae properties, Journal of Biomechanics Engineering 127/7 (2005) 1046-1053.
[68] H. Isaksson, S. Nagao, M. Małkiewicz, P. Julkunen, R. Nowak, J.S. Jurvelin, Precision of nanoindentation protocols for measurement of viscoelasticity in cortical and trabecular bone, Journal of Biomechanics 43 (2010) 2410-2417.
[69] G. Lewis, J.S. Nyman, The use of nanoindentation for characterizing the properties of mineralized hard tissues: state-of-the art review, Journal of Biomedical Material Research B: Applied Biomaterials 87/1 (2008) 286-301.
[70] J. Menclk, M.V. Swain, Errors associated with depth-sensing micro-indentation tests, Journal of Materials Research 10/6 (1995) 1491-1501.
[71] J. Nemecek, Nanoindentation in material science, Intech, 2012, http://dx.doi.org/10.5772/2829.
[72] J.Y. Rho, G.M. Pharr, Effects of drying on the mechanical properties of bovine femur measured by nanoindentation, Journal of Material Science: Materials in Medicine 10/8 (1999) 485-488.
[73] J.Y. Rho, T.Y. Tsui, G.M. Pharr, Elastic properties of human cortical and trabecular lamellar bone measured by nanoindentation, Biomaterials 18 (1997) 1325-1330.
[74] N. Rodriguez-Floreza, M.L. Oyen, S.J. Shefelbine, Insight into differences in nanoindentation properties of bone, Journal of the Mechanical Behaviour of Biomedical Materials 18 (2013) 90-99.
[75] J.G. Swadener, J.Y. Rho, G.M. Pharr, Effects of anisotropy on elastic moduli measured by nano-indentation in human tibial cortical bone, Journal of Biomedical Materials Research 57/1 (2001) 108-112.
[76] Z. Wu, T.A. Baker, T.C. Ovaert, G.L. Niebur, The Effect of Holding Time on Nanoindentation Measurements of Creep in Bone, Journal of Biomechanics 44/6 (2011) 1066-1072.
[77] P.K. Zysset, E. Guo, E. Hoffler, K.E. Moore, S.A. Goldstein, Elastic modulus and hardness of cortical and trabecular bone lamellae measured by nanoindentation in the human femur, Journal of Biomechanics 32 (1999) 1005-1012.